

1N-26
198085
374

NASA Technical Memorandum

NASA TM - 108431

MICROSTRUCTURAL STABILITY OF WROUGHT, LASER AND ELECTRON BEAM GLAZED NARLOY-Z ALLOY AT ELEVATED TEMPERATURES

By J. Singh, G. Jerman, B. Bhat, and R. Poorman

Materials and Processes Laboratory
Science and Engineering Directorate

N94-20100

Unclass

G3/26 0198085

November 1993

(NASA-TM-108431) MICROSTRUCTURAL
STABILITY OF WROUGHT, LASER AND
ELECTRON BEAM GLAZED NARLOY-Z ALLOY
AT ELEVATED TEMPERATURES (NASA)
37 p



National Aeronautics and
Space Administration

George C. Marshall Space Flight Center

REPORT DOCUMENTATION PAGE

Form Approved
OMB No. 0704-0188

Public reporting burden for this collection of information is estimated to average 1 hour per response, including the time for reviewing instructions, searching existing data sources, gathering and maintaining the data needed, and completing and reviewing the collection of information. Send comments regarding this burden estimate or any other aspect of this collection of information, including suggestions for reducing this burden, to Washington Headquarters Services, Directorate for Information Operations and Reports, 1215 Jefferson Davis Highway, Suite 1204, Arlington, VA 22202-4302, and to the Office of Management and Budget, Paperwork Reduction Project (0704-0188), Washington, DC 20503.

1. AGENCY USE ONLY (Leave blank)		2. REPORT DATE November 1993	3. REPORT TYPE AND DATES COVERED Technical Memorandum	
4. TITLE AND SUBTITLE Microstructural Stability of Wrought, Laser and Electron Beam Glazed NARloy-Z Alloy at Elevated Temperatures			5. FUNDING NUMBERS	
6. AUTHOR(S) J. Singh, G. Jerman, B. Bhat, and R. Poorman				
7. PERFORMING ORGANIZATION NAME(S) AND ADDRESS(ES) George C. Marshall Space Flight Center Marshall Space Flight Center, Alabama 35812			8. PERFORMING ORGANIZATION REPORT NUMBER	
9. SPONSORING / MONITORING AGENCY NAME(S) AND ADDRESS(ES) National Aeronautics and Space Administration Washington, DC 20546			10. SPONSORING / MONITORING AGENCY REPORT NUMBER NASA TM - 108431	
11. SUPPLEMENTARY NOTES Prepared by Materials and Processes Laboratory, Science and Engineering Directorate.				
12a. DISTRIBUTION / AVAILABILITY STATEMENT Unclassified—Unlimited			12b. DISTRIBUTION CODE	
13. ABSTRACT (Maximum 200 words) Microstructure of wrought, laser and electron-beam glazed NARloy-Z (Cu-3 wt.% Ag-0.5 wt.% Zr) was investigated for thermal stability at elevated temperatures (539 to 760 °C (1,100 to 1,400 °F)) up to 94 h. Optical and scanning electron microscopy and electron probe microanalysis were employed for studying microstructural evolution and kinetics of precipitation. Grain boundary precipitation and precipitate free zones (PFZ's) were observed in the wrought alloy after exposing to temperatures above 605 °C (1,120 °F). The fine-grained microstructure observed in the laser and electron-beam glazed NARloy-Z was much more stable at elevated temperatures. Microstructural changes correlated well with hardness measurements.				
14. SUBJECT TERMS laser glazing, electron beam glazing NARloy-Z, thermal stability			15. NUMBER OF PAGES 37	
			16. PRICE CODE NTIS	
17. SECURITY CLASSIFICATION OF REPORT Unclassified	18. SECURITY CLASSIFICATION OF THIS PAGE Unclassified	19. SECURITY CLASSIFICATION OF ABSTRACT Unclassified	20. LIMITATION OF ABSTRACT Unlimited	

WASH. STATE UNIVERSITY

TABLE OF CONTENTS

	Page
INTRODUCTION	1
EXPERIMENTAL PROCEDURE	2
RESULTS AND DISCUSSION	2
Hardness	2
Microstructural Evolution	3
SUMMARY	5
REFERENCES.....	6

PRECEDING PAGE BLANK NOT FILMED

LIST OF ILLUSTRATIONS

Figure	Title	Page
1a.	SSME MCC	7
1b.	Schematic of MCC cooling channels and hot wall	8
2.	Uniform microstructure in wrought NARloy-Z hot wall	9
3.	Microstructural changes in wrought NARloy-Z hot wall after hot firing and dog house formation	10
4.	Schematic line diagram of drop-through furnace	11
5.	Hardness change in wrought and laser-glazed NARloy-Z as a function of time at 593 °C (1,100 °F)	11
6.	Hardness change in wrought and laser-glazed NARloy-Z as a function of time at 649 °C (1,200 °F)	12
7.	Hardness change in wrought and laser-glazed NARloy-Z as a function of temperatures ranging from 593 to 760 °C (1,100 to 1,400 °F) for 24 h	12
8a.	Wrought NARloy-Z showing two-phase microstructure (intermetallic CuAgZr and Zr oxide) in Cu matrix	13
8b.	EPMA across the second phase in wrought NARloy-Z, showing Zr present as Zr ₂ O ₃ into Cu matrix	13
8c.	EPMA across the second phase in wrought NARloy-Z, showing Ag-rich intermetallic phases present into Cu matrix	14
8d.	EPMA across the second phase in wrought NARloy-Z, showing Zr-rich intermetallic phases present into Cu matrix	14
9.	Wrought NARloy-Z showing precipitation of second phases (intermetallic CuAgZr and Zr oxide) in Cu matrix after exposure at 593 °C (1,100 °F) for (a) 24, (b) 48, (c) 72, and (d) 94 h	15
10.	Wrought NARloy-Z showing grain boundary precipitation, PFZ near grain boundaries, and precipitation of second phases (intermetallic CuAg Zr and Zr oxide) in Cu matrix after exposure at 649 °C (1,200 °F) for (a) 24 and (b) 48 h	16

LIST OF ILLUSTRATIONS (continued)

Figure	Title	Page
11.	Optical (a: low magnification and b: high magnification) and SEM (c: low magnification and d: high magnification) micrographs of the wrought NARloy-Z showing grain boundary precipitation, PFZ near grain boundaries, and second-phase precipitation (intermetallic CuAg Zr and Zr oxide) in Cu matrix after exposure at 705 °C (1,300 °F) for 24 h	17
12.	EDS spectrum from precipitates (regions 1 and 2) and matrix (regions 4 and 6), as marked in figure 8c	18
13.	EPMA across precipitate, as marked in figure 11a.....	19
14.	Wrought NARloy-Z showing grain boundary precipitation, PFZ near grain boundaries, and second-phase precipitation (intermetallic CuAgZr and Zr oxide) in Cu matrix after exposure at 760 °C (1,400 °F) for (a) 24 and (b) 48 h.....	20
15.	Plot of PFZ width as a function of exposure to temperatures ranging from 649 to 760 °C (1,200 to 1,400 °C)	21
16.	Laser-glazed NARloy-Z showing uniform distribution of second phases in Cu matrix	21
17.	Laser-glazed NARloy-Z showing uniform distribution of second phases in Cu matrix after exposure at 593 °C (1,100 °F) for (a) 24, (b) 48, (c) 72, and (d) 84 h	22
18.	Laser-glazed NARloy-Z showing uniform distribution of faceted second phases in Cu matrix after exposure at 649 °C (1,200 °F) for (a) 24 and (b) 48 h	23
19.	EPMA across the faceted precipitate, as marked in figure 18	24
20.	Laser-glazed NARloy-Z showing uniform distribution of second phases in Cu matrix after 24 h at 649 °C (1,200 °F)	25
21.	EDS spectrum of precipitate and matrix from figure 20.....	26
22.	Laser-glazed NARloy-Z showing uniform distribution of second phases in Cu matrix after exposure at 760 °C (1,400 °F) for (a) 24 and (b) 48 h.....	27
23.	Electron beam-glazed NARloy-Z with uniform distribution of second phases in Cu matrix at a melt depth of ~0.6 mm (25 mils).....	28

LIST OF ILLUSTRATIONS (continued)

Figure	Title	Page
24.	Electron beam-glazed NARloy-Z showing uniform distribution of second phases in Cu matrix at melt depth of ~2 mm (80 mils).....	29
25.	Electron beam-glazed NARloy-Z showing uniform distribution of faceted second phases in Cu matrix after 24 h at (a) 705 °C (1,300 °F) and (b) 760 °C (1,400 °F)	30

TECHNICAL MEMORANDUM

MICROSTRUCTURAL STABILITY OF WROUGHT, LASER AND ELECTRON-BEAM GLAZED NARLOY-Z ALLOY AT ELEVATED TEMPERATURES

INTRODUCTION

Wrought NARloy-Z (Cu-3 wt.% Ag-0.5 wt.% Zr + traces of O₂, ~50 p/m) is now used to fabricate the main combustion chamber (MCC) liner (figs. 1a and 1b) for the space shuttle main engine (SSME). MCC liner construction is shown in figure 2. It consists of (A) hot wall, (B) channel lands, and (C) cooling channels. The hot wall thickness ranges from 0.5 to 0.75 mm (20 to 30 mils).

The present liner undergoes a heat treat cycle that includes solutionization in a vacuum furnace for 4 h at 935 °C (1,715 °F), water quenching to room temperature, and age hardening for 4 h at 480 °C (900 °F). This cycle produces a coarse-grained microstructure, with a Cu matrix that contains localized nonuniform distribution of Cu-Ag-Zr intermetallic phases and Zr oxides (fig. 2, regions A and B). The ductility of the liner is decreased by Ag- and Zr-rich phases at grain boundaries, which change fracture morphology from transgranular to intergranular.¹ These phases do not dissolve into the matrix by solutionizing heat treatment.²

The hot wall undergoes microstructural changes that include precipitation and coarsening of intermetallic phases in the matrix and grain boundaries (fig. 3). In wrought NARloy-Z, these inhomogeneities tend to lower the mechanical properties at temperatures above 315 °C (600 °F). Since the MCC liner is exposed to temperatures ranging from -252 °C to >540 °C (-422 to >1,000 °F) during hot fire, hot wall life is determined by the number of hot firings and the rate of microstructural degradation.

To ensure a service life of 300 cycles for the MCC liner, the chamber material must be capable of withstanding 1,200 cycles under normal operating conditions.³ However, service lives have been shorter than expected for the MCC liner. Failure analysis of the hot fired liner has shown that the operating temperature of the hot wall was much higher (>760 °C (1,400 °F)) than expected (538 °C (1,000 °F)). Failure analyses conducted by Morgan and Kobayashi⁴ and Sanders⁵ determined that the liner had failed by bursting or fracturing. The hot wall mechanical properties were degraded because of nonuniform microstructure, grain growth, grain boundary precipitation of intermetallic phases, and high temperature deformation that caused grain boundary coarsening and sliding. The hot wall bulged out between the cooling channels in response to high pressure inside the channels, thermal expansion, and temperatures above 538 °C (1,000 °F) outside the hot wall (referred to as "dog house"). In addition, oxidation/reduction reaction with Cu (known as "blanching") was observed. Blanching was characterized by subsurface wormholing, which interconnected and formed longitudinal cracks, and increased hot wall surface roughness.^{3,4} In blanching areas, the surface temperature was near 1,085 °C (1,985 °F), with substrate temperatures that exceeded 926 °C (1,700 °F).³ The local heat transfer coefficient had increased with hot wall roughness, which caused operating temperatures to rise well above the maximum design temperature.

Three different approaches can be taken to increase the service life of the MCC liner. One approach is to develop a new liner alloy with higher thermal stability, better mechanical properties, and

improved thermal conductivity.³ A second approach is to apply thermal barrier coatings such as NiCrAlY, TiN, etc., to the liner to lower the operating temperatures. A third approach is to improve the microstructure and thermal stability of the wrought NARloy-Z liner by surface glazing. This report presents the third approach which is a relatively new technique in which the surface is rapidly melted and resolidified with a high-energy laser or electron beam. The glazed area develops a fine-grained microstructure with a uniform distribution of second phases in the matrix that is much more stable at elevated temperatures.

EXPERIMENTAL PROCEDURE

Wrought NARloy-Z was selected as a starting material for laser and electron-beam (EB) glazing. The samples of wrought NARloy-Z were solutionized at 935 °C (1,715 °F) before studying the precipitation kinetics. Specimens of wrought, laser, and EB glazed NARloy-Z were exposed to elevated temperatures ranging from 593 to 760 °C (1,100 to 1,400 °F) for up to 84 h in a drop-through furnace (fig. 4) to effect microstructural changes and then rapidly quenched with helium gas. Metallographic samples were then prepared and etched with an ammonium persulphate solution ((NH₄)₂S₂O₈ per 100 mL H₂O). Vicker hardness measurements were made with a 200-g weight for the purpose of comparison of microstructure with hardness. The samples were examined with an optical microscope, a Hitachi S-4000 field emission scanning electron microscope (SEM), and a Cameca SX-50 electron microprobe. Elemental analyses of different phases were performed using qualitative energy dispersive spectroscopy (EDS) and electron probe microanalysis (EPMA).

RESULTS AND DISCUSSION

Hardness

The hardness change in wrought and laser-glazed NARloy-Z, as a function of exposure time up to 84 h at 593 °C (1,100 °F), is shown in figure 5 and at 649 °C (1,200 °F) in figure 6. There was some drop in the hardness of the laser-glazed NARloy-Z as compared to the wrought alloy after exposing at 593 °C (1,100 °F) for up to 84 h. At 649 °C (1,200 °F), hardness values remained constant for up to 24 h and then dropped slowly by ~7 percent as a function of time (fig. 6). Figure 7 shows hardness changes as a function of temperature from 593 to 760 °C (1,100 to 1,400 °F) for a constant exposure time (24 h).

The hardness of EB-glazed NARloy-Z was measured before and after exposure at 705 °C (1,300 °F) for 24 h. The hardness values were similar to the laser-glazed alloy. Andrus and Boedean³ also obtained comparable values when they measured the hardness of wrought and EB-processed NARloy-Z.

The average hardness of laser-glazed NARloy-Z was approximately 15 percent higher than the wrought alloy and remained so even after exposing to elevated temperatures ranging from 593 to 760 °C (1,100 to 1,400 °F), as shown in figures 5 to 7. Increased hardness was probably due to the fine-grained microstructure and uniform distribution of the second phase in the Cu matrix. This subject will be discussed further in the next section.

Microstructural Evolution

Wrought NARloy-Z. In general, the wrought NARloy-Z starting material had a coarse-grained microstructure (fig. 8a) with an uneven distribution of secondary precipitates. Microprobe analyses showed that Zr was present, probably as Zr oxide Zr_2O_3 (fig. 8b). Ag- and Zr-rich intermetallic phases were present in the Cu matrix (figs. 8c and 8d). In addition, oxides of Ag and Cu were present in the matrix. The secondary phases varied in size from 1 to 10 μm . The average grain size was approximately 150 μm . Figure 9 shows precipitation and coarsening in the Cu matrix and at the grain boundaries after exposure to 593 °C (1,100 °F) for up to 94 h. Figure 10 shows the microstructural changes in NARloy-Z after exposure to 649 °C (1,200 °F) up to 48 h. Precipitate-free zones (PFZ's) were observed near the grain boundaries and large intermetallic phases as shown by arrows in figure 10. The size of precipitates and PFZ width increased at 649 °C (1,200 °F) as exposure time increased from 24 to 48 h. After 24 h exposure at 649 °C (1,200 °F), the volume fraction and size of precipitates in the Cu matrix (fig. 10b) were noticeably larger than those in the starting material. The same was true for NARloy-Z exposed to 594 °C (1,100 °F) for ~94 h (fig. 9).

After 24 h exposure at 705 °C (1,300 °F), the wrought NARloy-Z showed relatively large intermetallic precipitates in the Cu matrix and grain boundaries (fig. 11). The PFZ width was also larger than that exposed to 649 °C (1,200 °F) for 48 h (compare figs. 10 and 11). EDS analysis was used to identify the matrix and grain-boundary precipitates as Ag- and Zr-rich intermetallic phases (fig. 12), and an EPMA was carried out across the grain boundary (line AB as shown in fig. 11a) to confirm the analysis. No concentration gradient of Zr and Ag solute atoms was observed across the PFZ and grain boundary (fig. 13), indicating that the precipitation reaction was essentially complete.

After exposure at 760 °C (1,400 °F) up to 48 h, the wrought NARloy-Z showed even coarser precipitation of intermetallic phases (fig. 14). The PFZ width was also larger than the NARloy-Z exposed to 649 to 705 °C (1,200 to 1,300 °F).

Two significant features are noteworthy in the wrought NARloy-Z exposed from 593 to 760 °C (1,100 to 1,400 °F): (a) precipitation and coarsening of Ag- and Zr-rich intermetallic phases in the matrix and at grain boundaries and (b) PFZ's near large intermetallic phases and at grain boundaries (figs. 10 to 14).

At temperatures above 649 °C (1,200 °F), PFZ formation probably occurred in response to grain boundary precipitation, migration, and long-range solute atom diffusion. The PFZ width increased as a function of temperature (fig. 15). Extrapolation of the PFZ size to zero in figure 15 indicates that PFZ occurs only above 605 °C (1,120 °F). The prior investigation⁶ was conducted below 538 °C (1,000 °F), which may be why the investigators did not report PFZ formation in wrought NARloy-Z.

When microstructure and hardness measurements were compared, good correlation was obtained between the two. Hardness decreased as the exposure temperatures increased from 649 to 760 °C (1,200 to 1,400 °F), probably due to rapid depletion of Ag and Zr solute atoms from the matrix and coarsening of intermetallic phases in the Cu matrix (figs. 5 to 7).

Laser and Electron-Beam Glazed NARloy-Z. Metallographic examination of laser-glazed NARloy-Z revealed uniform distribution of second phases in the Cu matrix (fig. 16). No grain boundary segregation was observed. In the rapidly solidified region, the average grain size was 100 μm , which is about half the wrought NARloy-Z grain size (150 to 300 μm). No significant change in the microstructure was observed on exposure at 593 °C (1,100 °F) for up to 84 h (fig. 17). A small amount of

coarsening of the second phase was observed as a function of time. Further coarsening of second phases was observed after exposing at 649 °C (1,200 °F) for up to 48 h (figs. 18a and 18b). These precipitates were aligned and had a faceted morphology (fig. 18b). However, the second phase sizes were still small and averaged less than 0.5 μm, smaller than those observed in wrought NARloy-Z (10 μm, fig. 8).

The EPMA technique was used to determine the concentration profile across the aligned precipitate (figs. 18 and 19). Faceted precipitates were mostly Ag, whereas most of the Zr was found in the matrix (fig. 19). The second phases coarsened further on exposures to higher temperatures, 705 to 760 °C (1,300 to 1,400 °F), but the average size was still small and remained at less than 0.5 μm (figs. 20 and 22). Unlike the wrought NARloy-Z, grain boundary precipitation and PFZ's were not observed in the Cu matrix in any of the experiments.

EB-glazed NARloy-Z showed a fine-grained microstructure (fig. 23) that is comparable to laser-glazed NARloy-Z (fig. 16). The melt pool ranged in depth from 0.6 to 2 mm (25 to 80 mils), depending upon processing conditions such as traverse speed and beam current (fig. 24).

Faceted and aligned precipitates were observed in the Cu matrix of EB-glazed samples exposed to 704 to 760 °C (1,300 to 1,400 °F) for up to 48 h (fig. 25). The second phase averaged less than 0.5 μm in size. No significant differences were seen in the microstructure of EB-processed and laser-glazed samples exposed to temperatures from 649 to 769 °C (1,200 to 1,400 °F).

Laser-glazed NARloy-Z was always harder than the wrought alloy by 15 percent or more (fig. 5). The higher hardness of the laser-glazed alloy was probably due to small-grained microstructure, fine and uniform distribution of the second phase in the Cu matrix, and the absence of PFZ and/or grain boundary precipitations. Its overall microstructure remained the same even after exposure to high temperature, with the exception of slight coarsening of the second phase. The wrought alloy, on the other hand, was constituted of a microstructure that was significantly changed by exposure to high temperatures (figs. 10 to 14). The high thermal stability of laser-glazed NARloy-Z is due to the short diffusion distance of solute atoms (i.e., separation between precipitates is small). This feature also prevents precipitation at the grain boundaries. The laser-glazed and EB-glazed alloys also underwent rapid melting and solidification, resulting in an extended solid solubility of Zr solute atoms into the Cu matrix.

In wrought NARloy-Z, Zr is introduced to suppress discontinuous precipitation and to absorb oxygen by forming Zr_2O_3 . At high temperatures, Zr_2O_3 is believed to improve mechanical properties by preventing grain growth.⁵ The wrought alloy contained Zr_2O_3 as well as Ag- and Zr-rich intermetallic phases. The actual microstructure consisted of relatively large grains with nonuniform distribution of intermetallic Zr- and Ag-rich phases (fig. 9). These microstructural features contribute to lower mechanical properties at elevated temperatures >538 °C (1,000 °F). In particular, the large grain size lowers ductility.¹

Under equilibrium conditions, the maximum solid solubility of Zr is about 0.15 wt.% in the Cu matrix at ~822 °C (1,512 °F), decreasing as temperature decreases. NARloy-Z contains about 0.5 wt.% Zr and the excess Zr precipitates either as Zr-rich an intermetallic phase or as Zr oxide. Inherent rapid melting and solidification, which occurred in the laser- and EB-glazing processes, created a nonequilibrium condition, thereby extending the solid solubility of Zr in the copper matrix. The atomic size of Zr (0.162 nm) is larger (~30 percent) than the Cu matrix (0.1278 nm). Due to the extended solid solubility of Zr atoms, the lattice strain was developed in the Cu matrix, which probably changed the kinetics of Ag precipitation (compare figs. 10b and 18b). Ag precipitated as elemental Ag in laser-glazed NARloy-Z, whereas Ag- and Zr-rich intermetallic precipitates were observed in the wrought alloy (figs. 13 and

19). The Ag and Zr alloying additions appear to play different roles in the wrought NARloy-Z versus the laser-glazed or EB-processed alloys, although all three forms retained the overall Cu-3 percent Ag-0.5 percent Zr composition.

In the laser- and EB-glazed alloys, Zr is present in the Cu matrix as solid solution and appears to stay in the matrix up to 760 °C (1,400 °F) and does not precipitate out. These factors probably contribute to their higher microstructural stability, higher hardness, and enhanced thermal stability (figs. 5 to 7). Therefore, the EB- or laser-glazing approach can be used to enhance the life of the SSME-MCC or another advanced MCC which uses NARloy-Z as liner material.

SUMMARY

Microstructural evolution and precipitation morphology were investigated in wrought, laser-, and EB-glazed NARloy-Z samples by exposing them to temperatures from 593 to 760 °C (1,100 to 1,400 °F). The results are summarized below and are applicable to a NARloy-Z MCC liner.

Wrought Alloy

1. Large-grained microstructure (150 to 300 μm) has 15-percent lower hardness than the laser-glazed alloy.
2. Zr- and Ag-rich intermetallic phases were observed at grain boundaries and in the Cu matrix after exposure to temperatures above 593 °C (1,100 °F).
3. Nonuniform microstructure and PFZ's were formed after exposure to temperatures above 605 °C (1,120 °F).

Laser- and EB-Glazed NARloy-Z

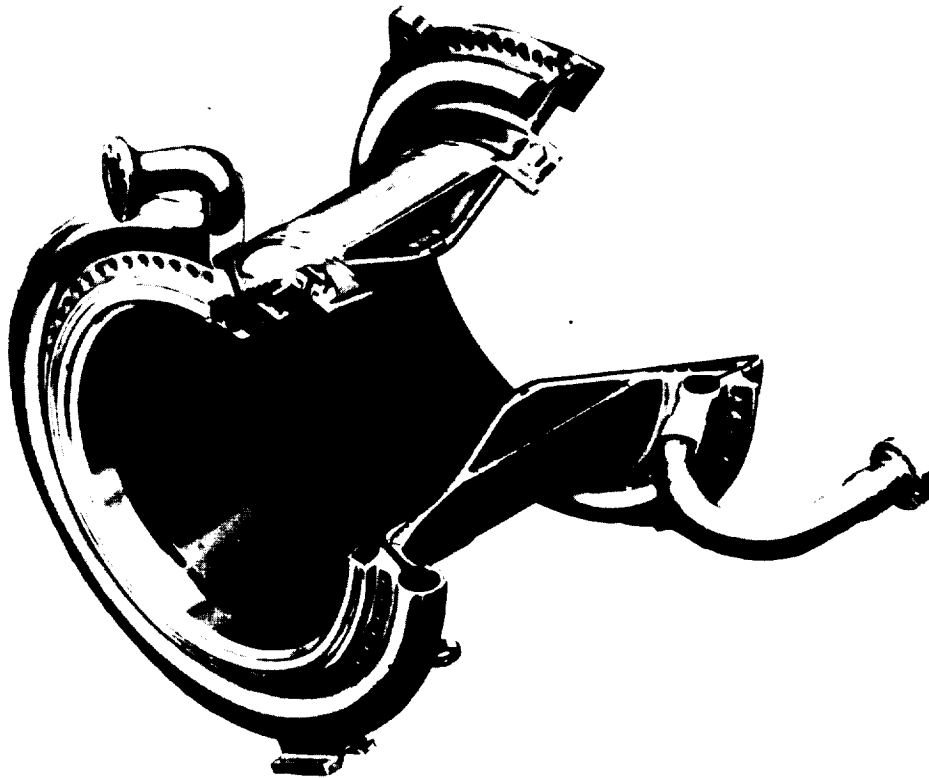
1. The hardness of laser- or EB-glazed NARloy-Z was approximately 15-percent higher than the wrought alloy and remained higher even after long exposures to elevated temperatures up to 760 °C (1,400 °F). The higher hardness was due to fine-grained microstructure (50 to 100 μm) with uniform distribution of the second phase in the matrix.
2. Grain-boundary precipitation and PFZ were not observed.
3. Extended solid solubility of Zr in the Cu matrix probably contributed to solid solution strengthening, which changed the Ag precipitation and coarsening kinetics to an aligned faceted morphology.
4. The microstructure was thermally stable up to 760 °C (1,400 °F).

Recommendation

Future MCC design should be cognizant of the thermal effects on NARloy-Z as discussed in this report. Further, beam glazing of the MCC liner should be pursued to enhance its service life.

REFERENCES

1. Chen, P.S., and Sanders, J.H.: "An Investigation on the Ductility Loss of VPS NARloy-Z at Elevated Temperatures." IIT Research Institute/MRF, 1992.
2. Singh, J.S., Jerman, G., Poorman, R., and Bhat, B.N.: "Microstructural Evolution of NARloy-Z at Elevated Temperatures." Marshall Space Flight Center, 1993.
3. Andrus, J.S., and Boedeau, R.G.: "Thrust Chamber Material Technology Program." Pratt and Whitney, 1989.
4. Morgan, D.B., Kobayashi, A.C.: "Main Combustion Chamber and Cooling Technology." Aerojet, 1989.
5. Sanders, J.S.: "An Investigation of Main Combustion Chamber Liner 4011 Degradation." IIT Research Institute/Metallurgy Research Facility, 1992.
6. Paton, N.E., and Robertson, W.M.: "Metallurgy of NARloy-Z." Rocketdyne, March 1973.



GEOMETRY

- NARLOY Z LINER + EDCu BARRIER + EDNi CLOSE-OUT + INCO 718 STRUCTURE SHELL
- NUMBER OF SLOTS 390
- NUMBER OF ACOUSTIC CAVITIES 30
- INJECTOR END DIAMETER 17.74 IN.
- THROAT AREA 83.41 IN.²
- INJECTOR END TO THROAT LENGTH 14.00 IN.
- CONTRACTION RATIO 2.96:1
- EXPANSION RATIO 5.0:1

OPERATING PARAMETERS (RPL, MR-6.0)

- THROAT STAGNATION PRESSURE 3009 PSIA
- COOLANT INLET PRESSURE 5949 PSIA
- COOLANT INLET TEMPERATURE 96 R
- COOLANT EXIT PRESSURE 4543 PSIA
- COOLANT EXIT TEMPERATURE 477 R
- COOLANT FLOWRATE 26.75 LB/SEC
- HOT GAS WALL TEMPERATURE AT THROAT 1000 F

Figure 1a. SSME MCC.

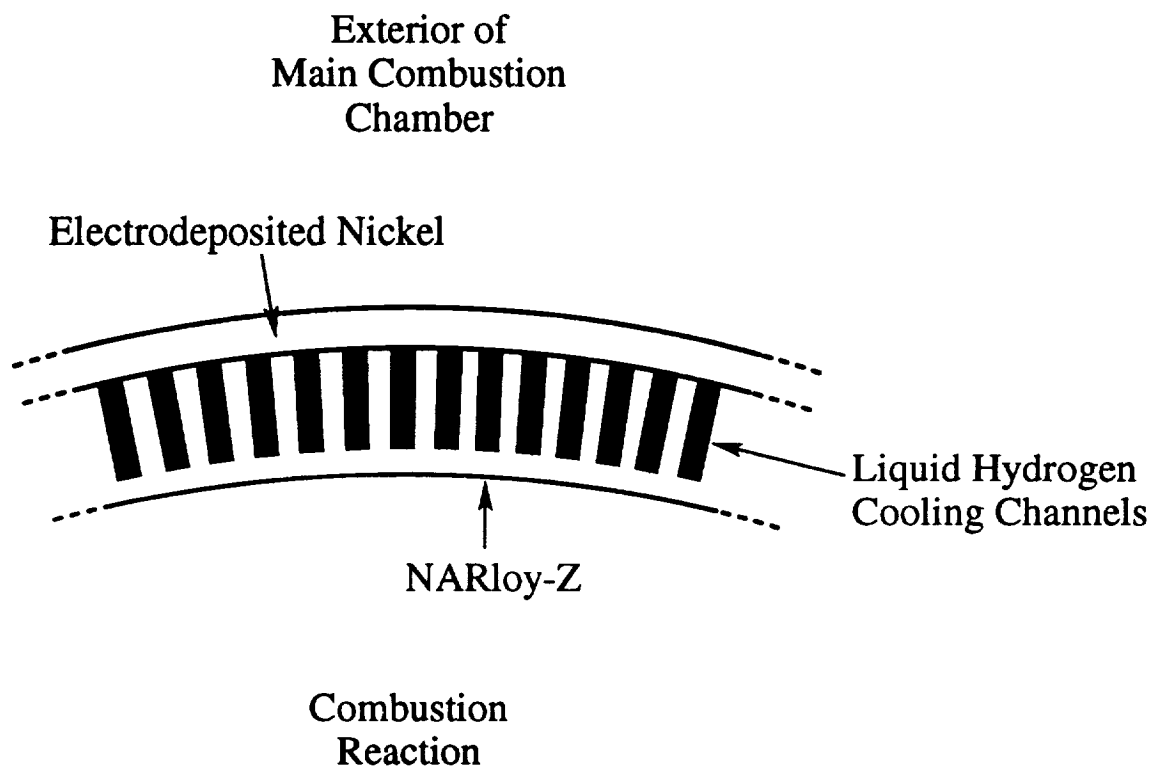
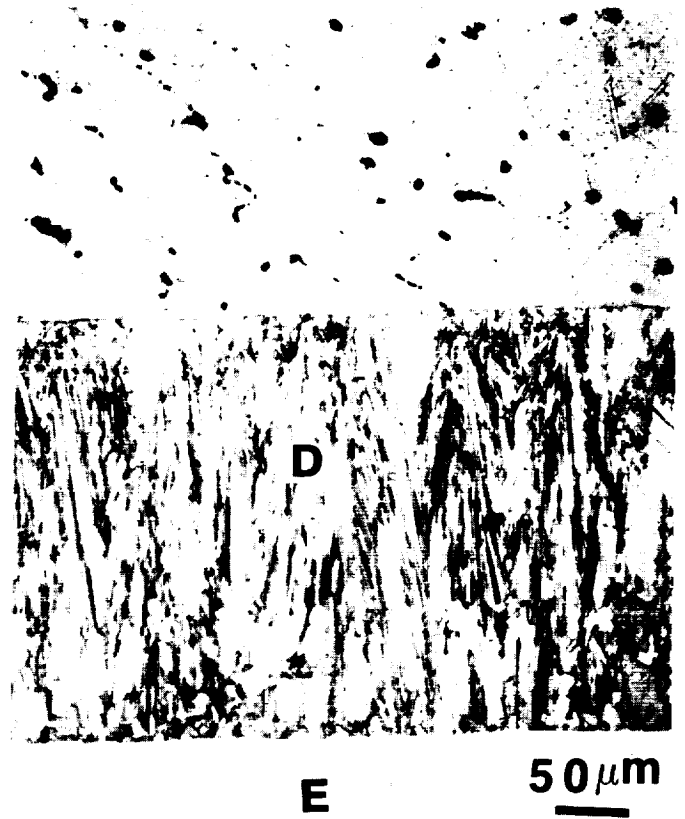
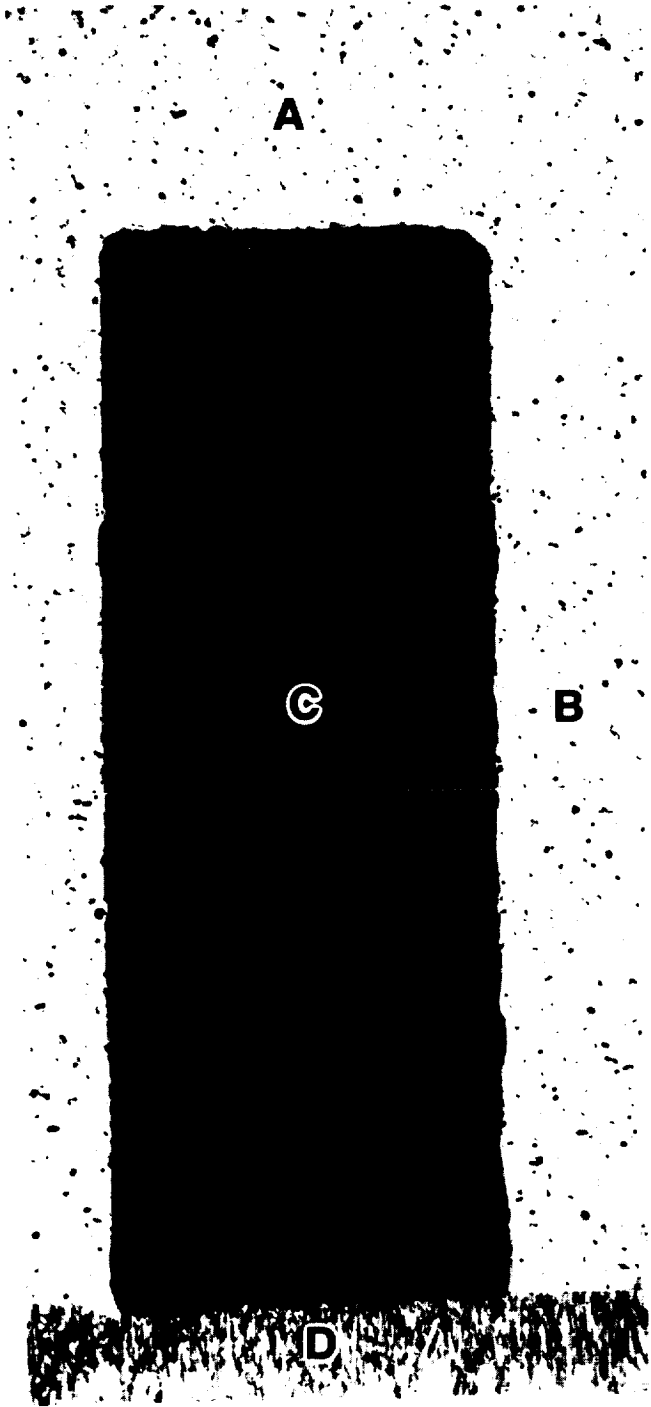


Figure 1b. Schematic of MCC cooling channels and hot wall.

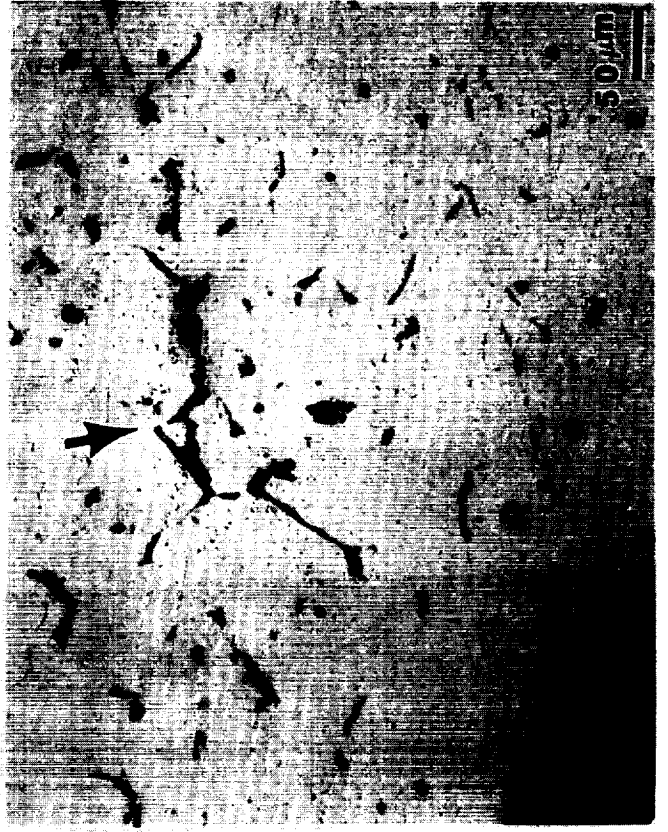


- A – Hot wall
- B – Channel land
- C – Cooling channels
- D – Cold wall (ED Cu)
- E – Electrodeposited Ni

Figure 2. Uniform microstructure in wrought NARloy-Z hot wall.



a



b

Figure 3. Optical micrographs of microstructural changes in the hot wall (region A) after hot firing.

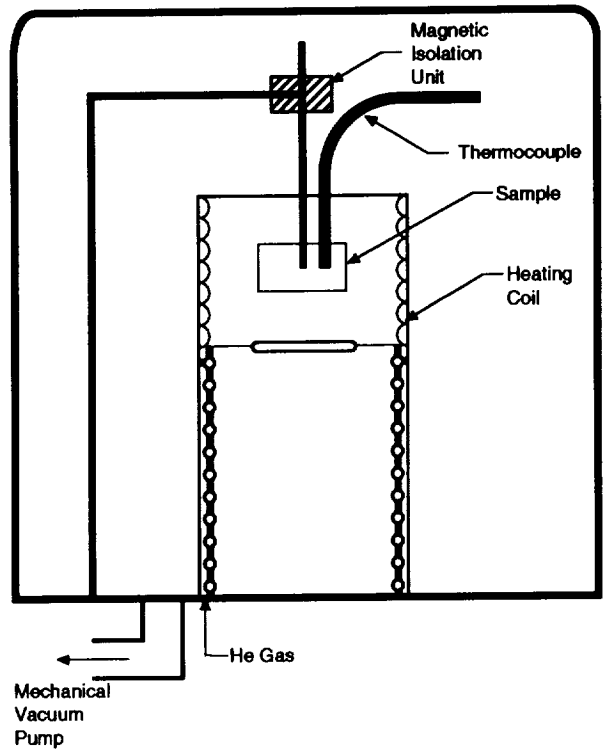


Figure 4. Schematic line diagram of drop-through furnace.

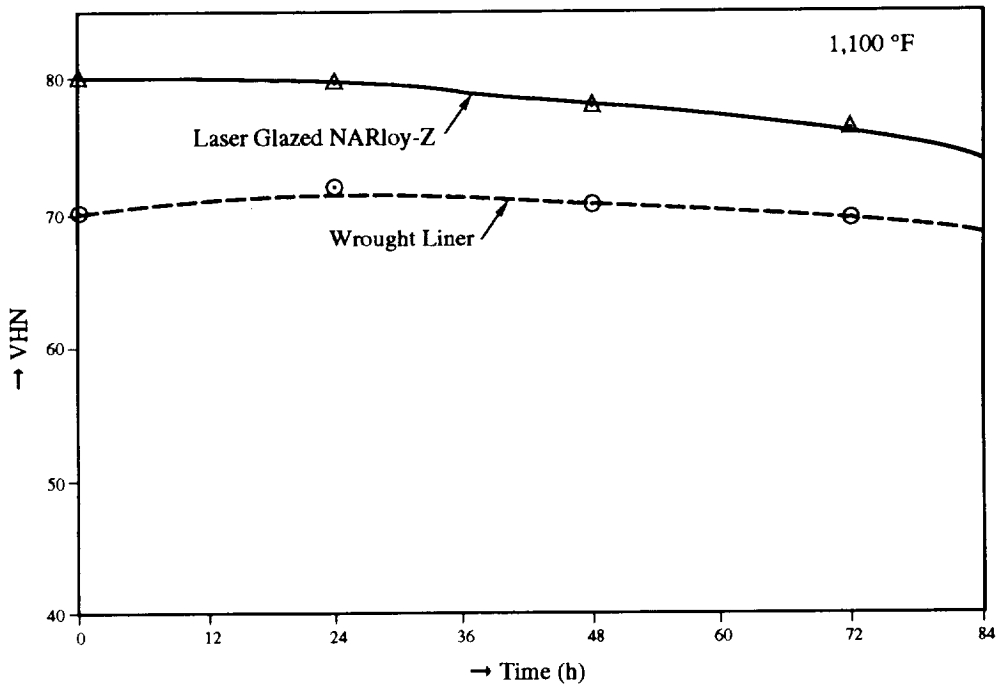


Figure 5. Hardness change in wrought and laser-glazed NARloy-Z as a function of time at 593 °C (1,100 °F).

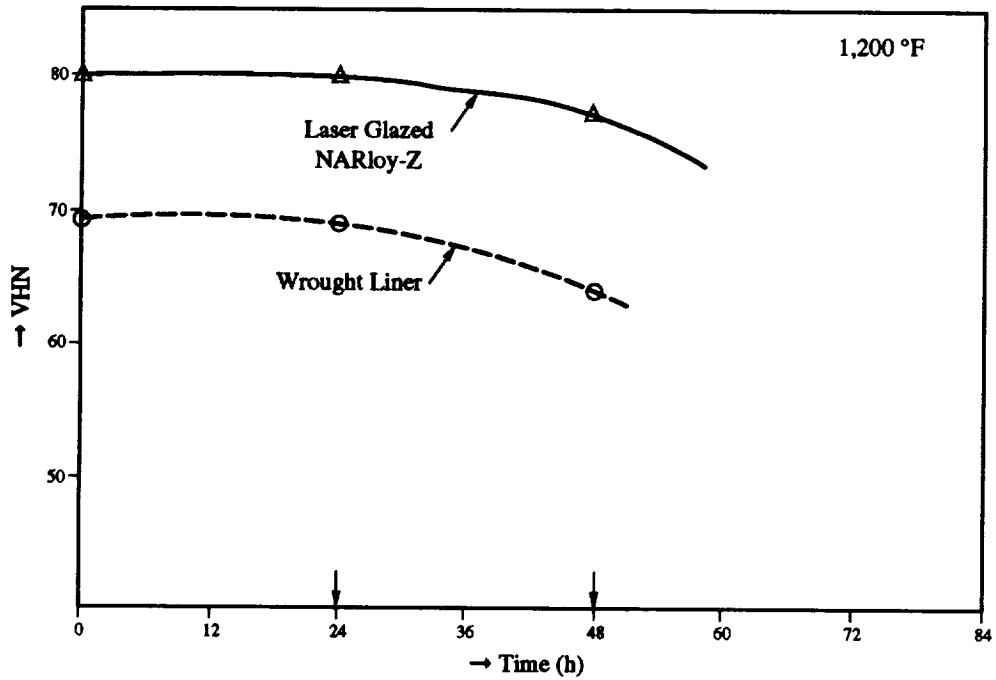


Figure 6. Hardness change in wrought and laser-glazed NARloy-Z as a function of time at 649 °C (1,200 °F).

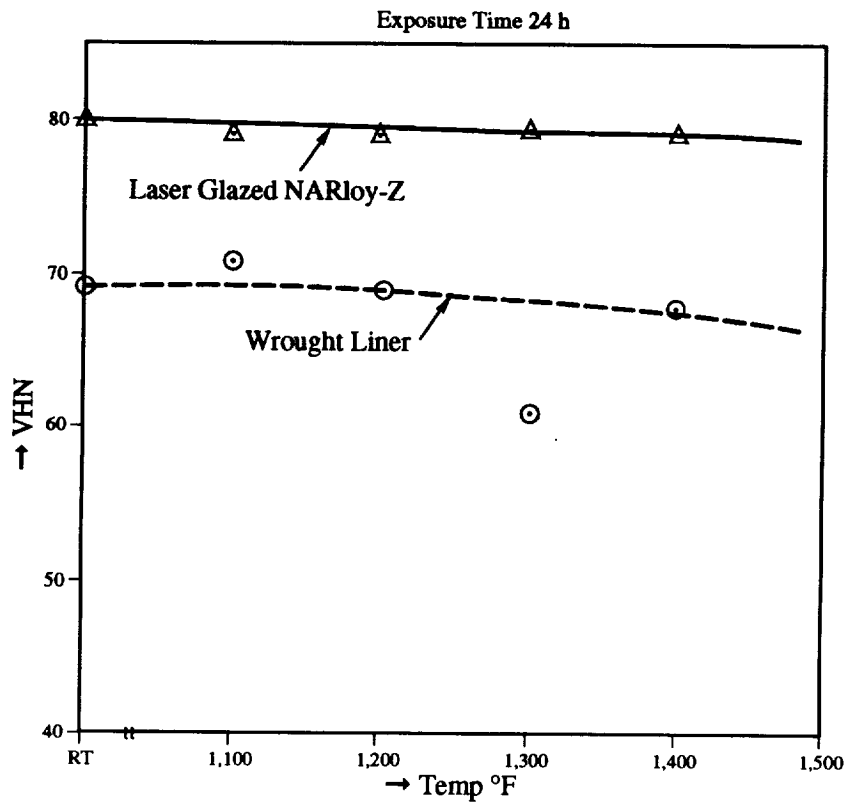


Figure 7. Hardness change in wrought and laser-glazed NARloy-Z as a function of temperatures ranging from 593 to 760 °C (1,100 to 1,400 °F) for 24 h.

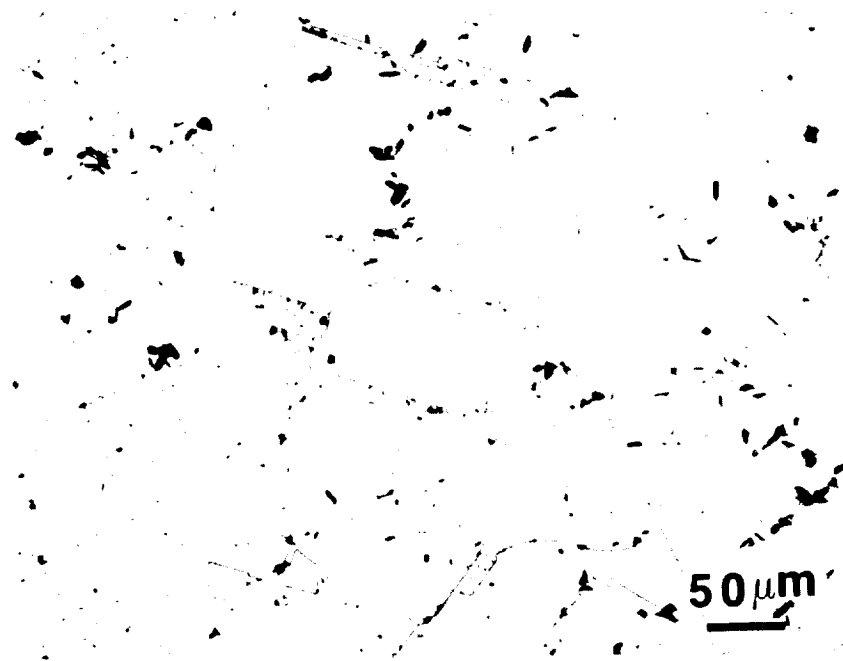


Figure 8a. Wrought NARloy-Z showing two-phase microstructure (intermetallic CuAgZr and Zr oxide) in Cu matrix.

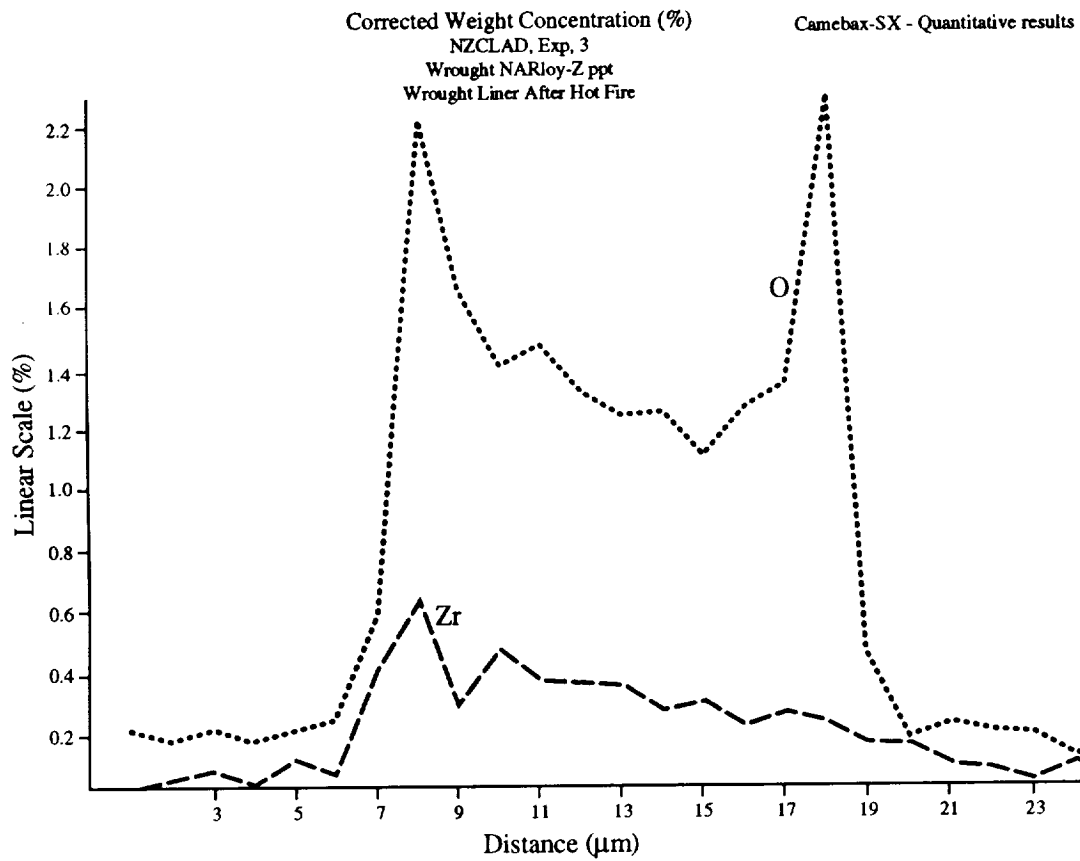


Figure 8b. EPMA across the second phase in wrought NARloy-Z, showing Zr present as Zr_2O_3 into Cu matrix.

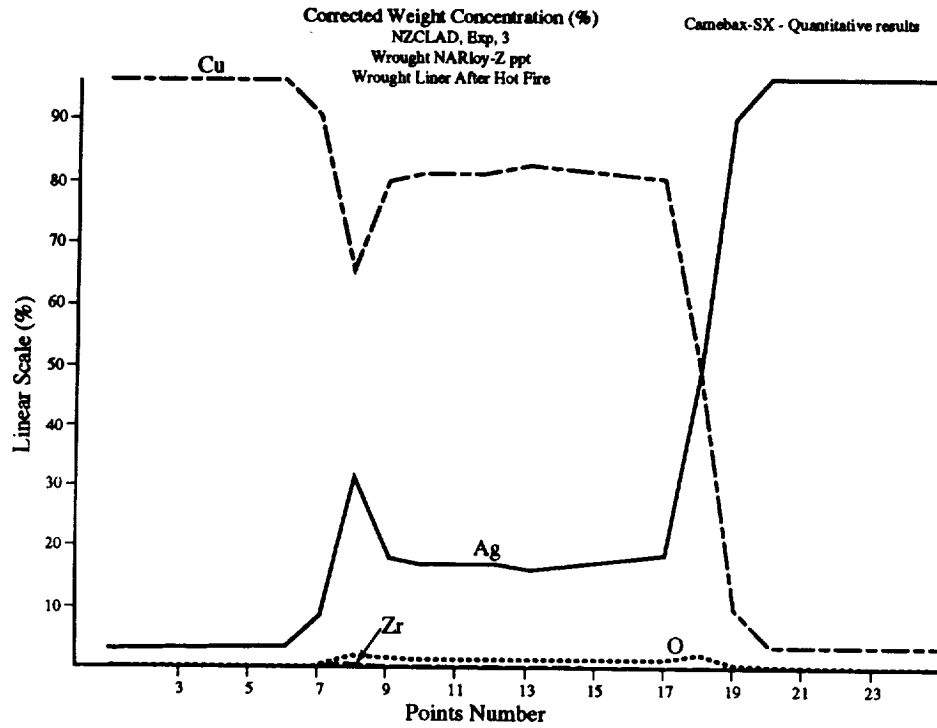


Figure 8c. EPMA across the second phase in wrought NARloy-Z, showing Ag-rich intermetallic phases present into Cu matrix.

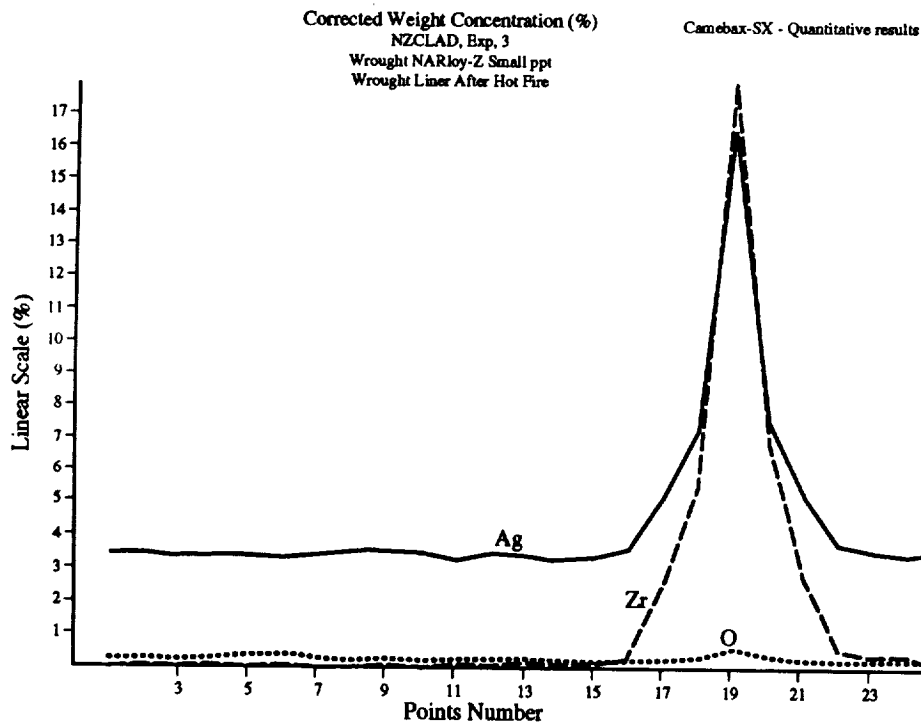


Figure 8d. EPMA across the second phase in wrought NARloy-Z, showing Zr-rich intermetallic phases present into Cu matrix.



Figure 9. Wrought NARloy-Z showing precipitation of second phases (intermetallic CuAgZr and Zr oxide) in Cu matrix after exposure at 593 °C (1,100 °F) for (a) 24, (b) 48, (c) 72, and (d) 94 h.

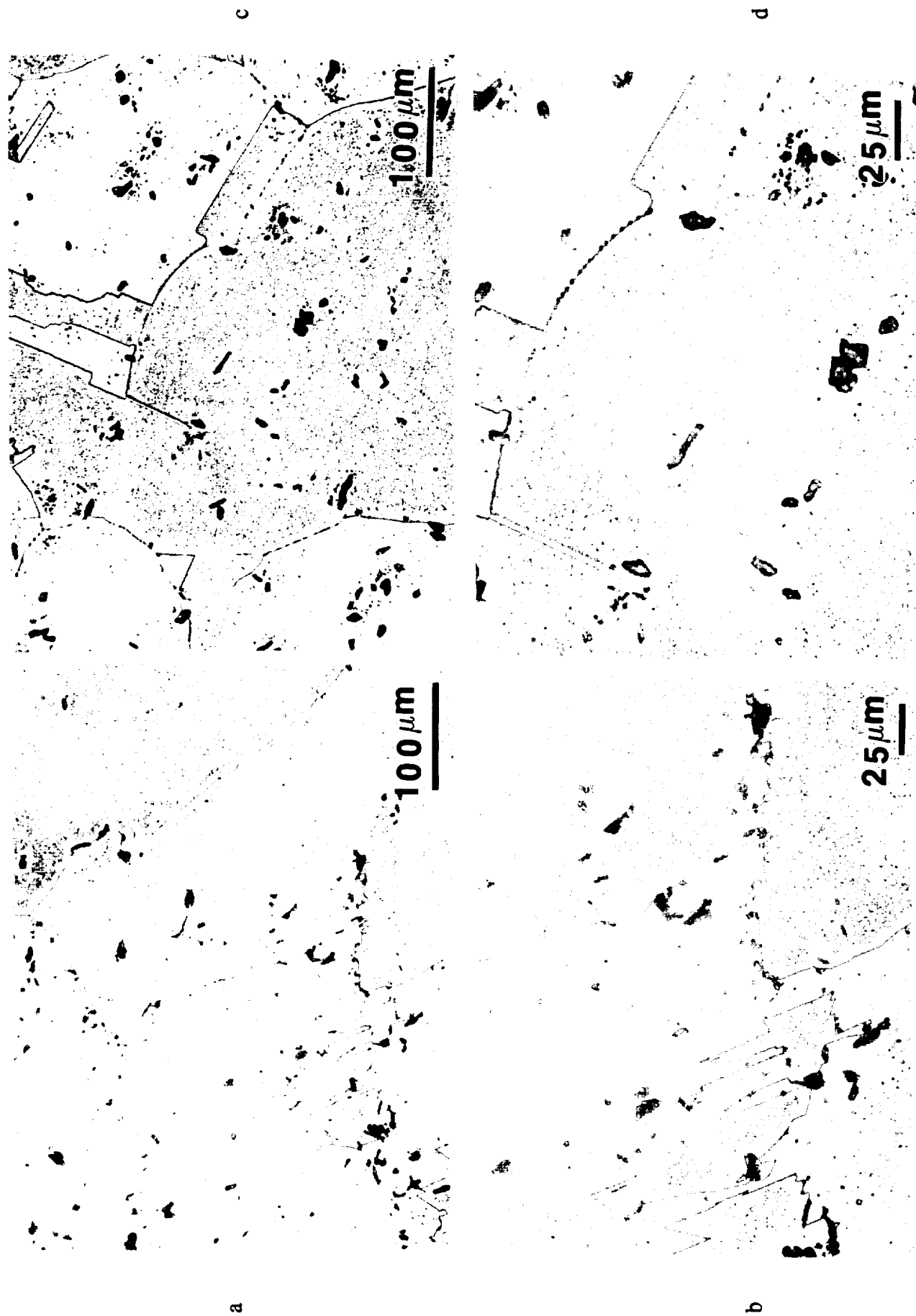


Figure 10. Wrought NARloy-Z showing grain boundary precipitation, PFZ near grain boundaries, and precipitation of second phases (intermetallic CuAgZr and Zr oxide) in Cu matrix after exposure at 649 °C (1,200 °F) for (a) 24 and (b) 28 h.

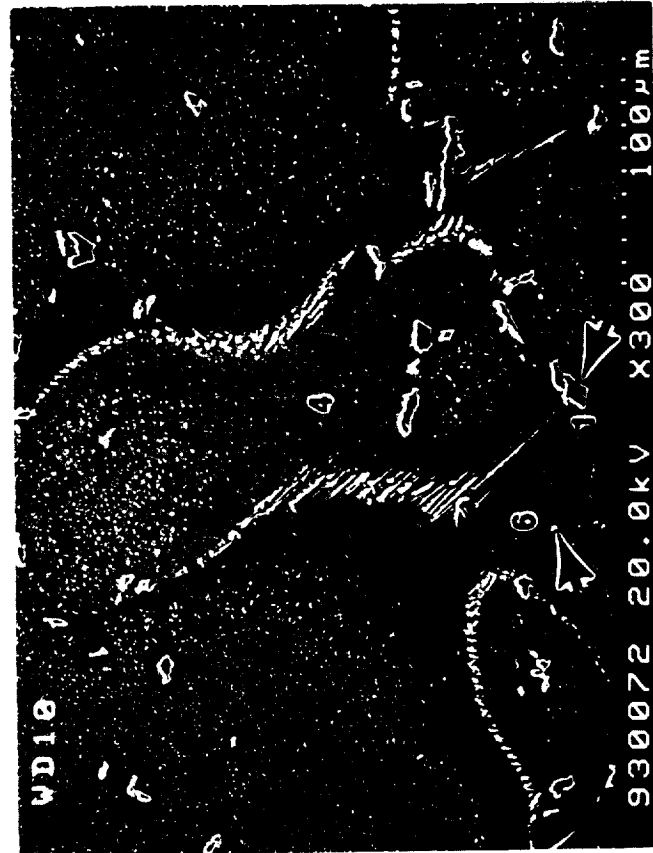


Figure 11. Optical (a: low magnification and b: high magnification) and SEM (c: low magnification and d: high magnification) micrographs of the wrought NARloy-Z showing grain boundary precipitation, PFZ near grain boundaries, and second-phase precipitation (intermetallic CuAgZr and Zr oxide) in Cu matrix after exposure at 705 °C (1,300 °F) for 24 h.

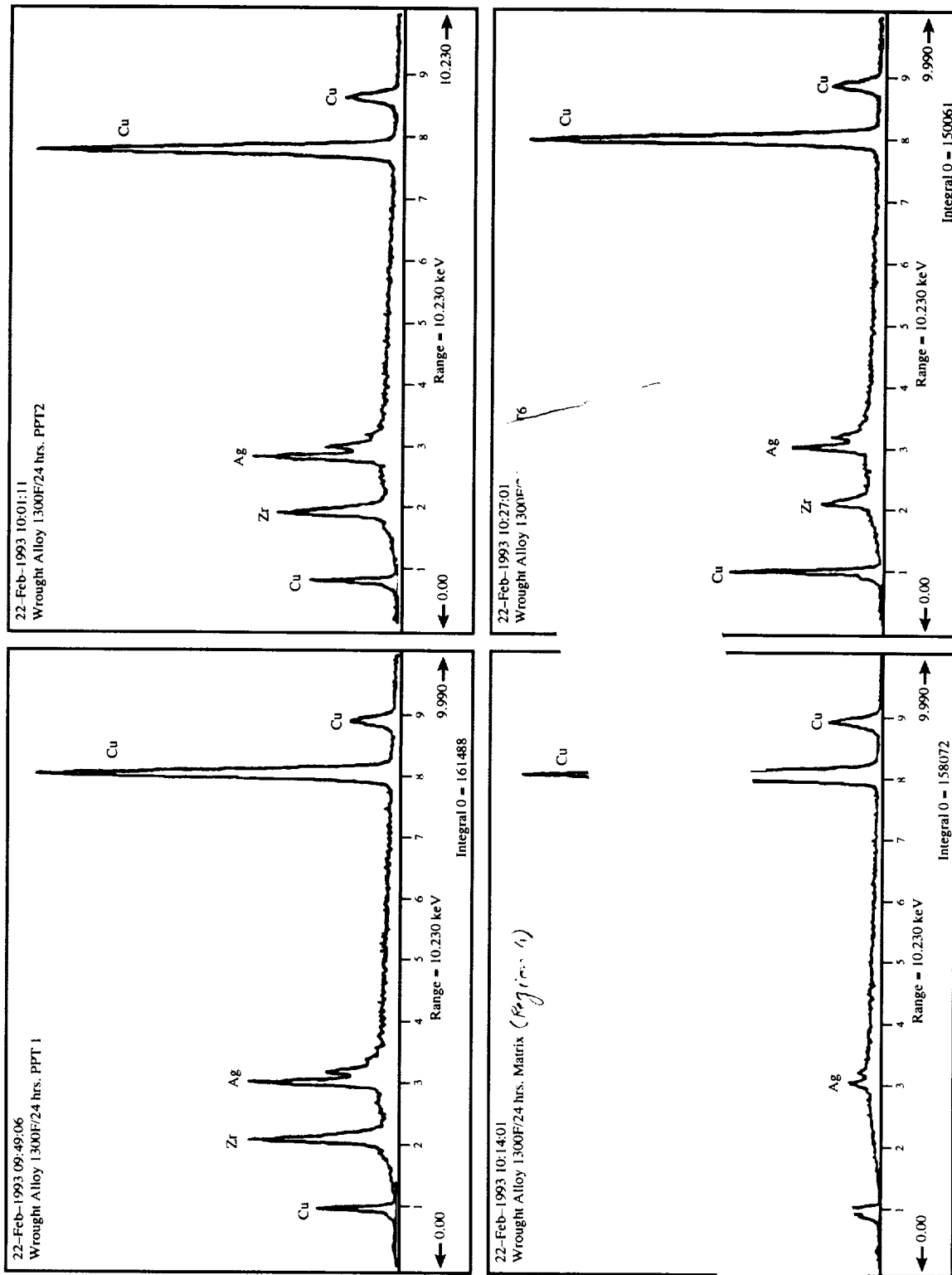


Figure 12. EDS spectrum from precipitates (regions 1 and 2) and matrix (regions 4 and 6), as marked in figure 8c.

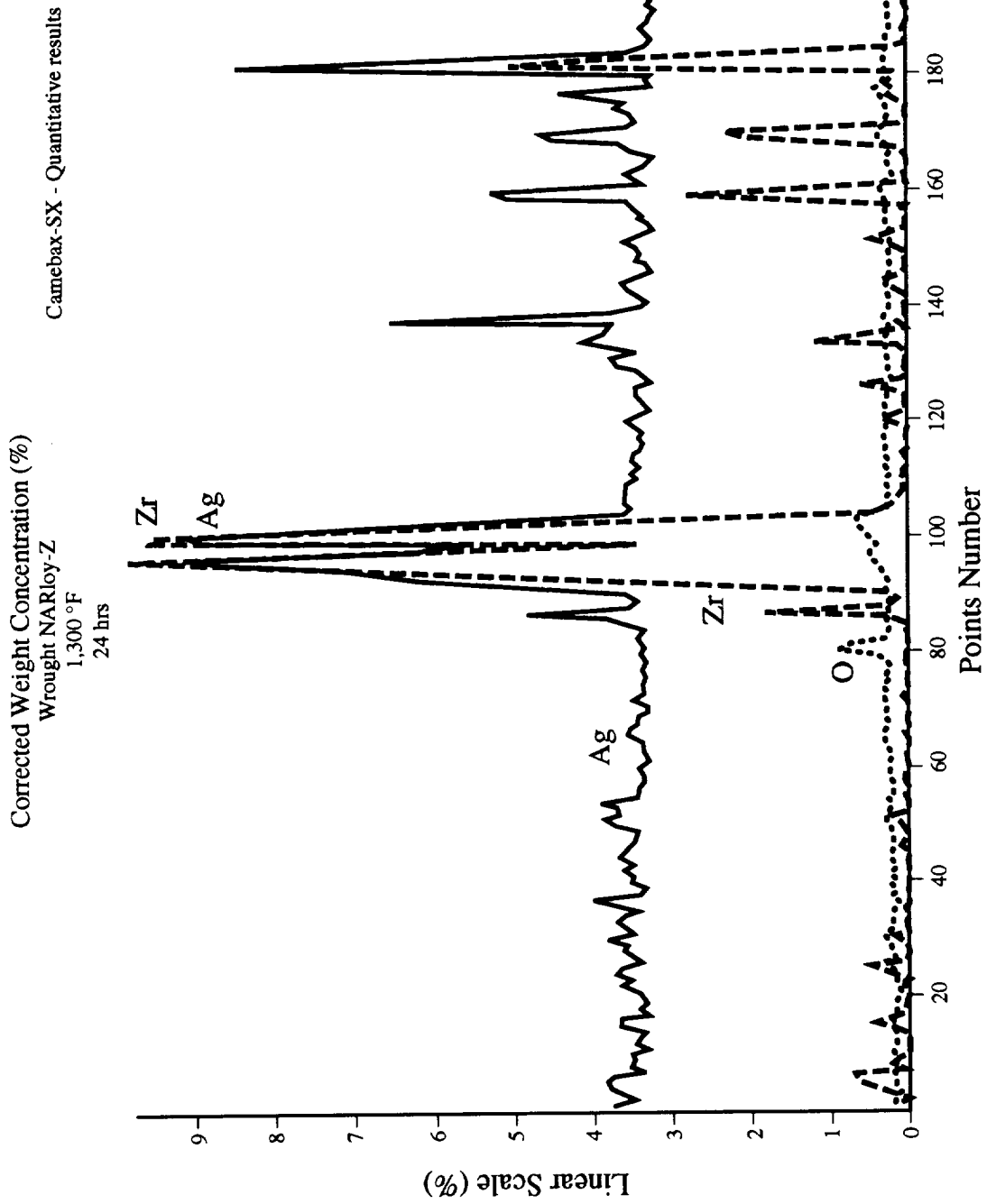


Figure 13. EPMA across precipitate, as marked in figure 11a.



Figure 14. Wrought NARloy-Z showing grain boundary precipitation, PFZ near grain boundaries, and second-phase precipitation (intermetallic CuAgZr and Zr oxide) in Cu matrix after exposure at 760 °C (1,400 °F) for (a) 24 and (b) 48 h.

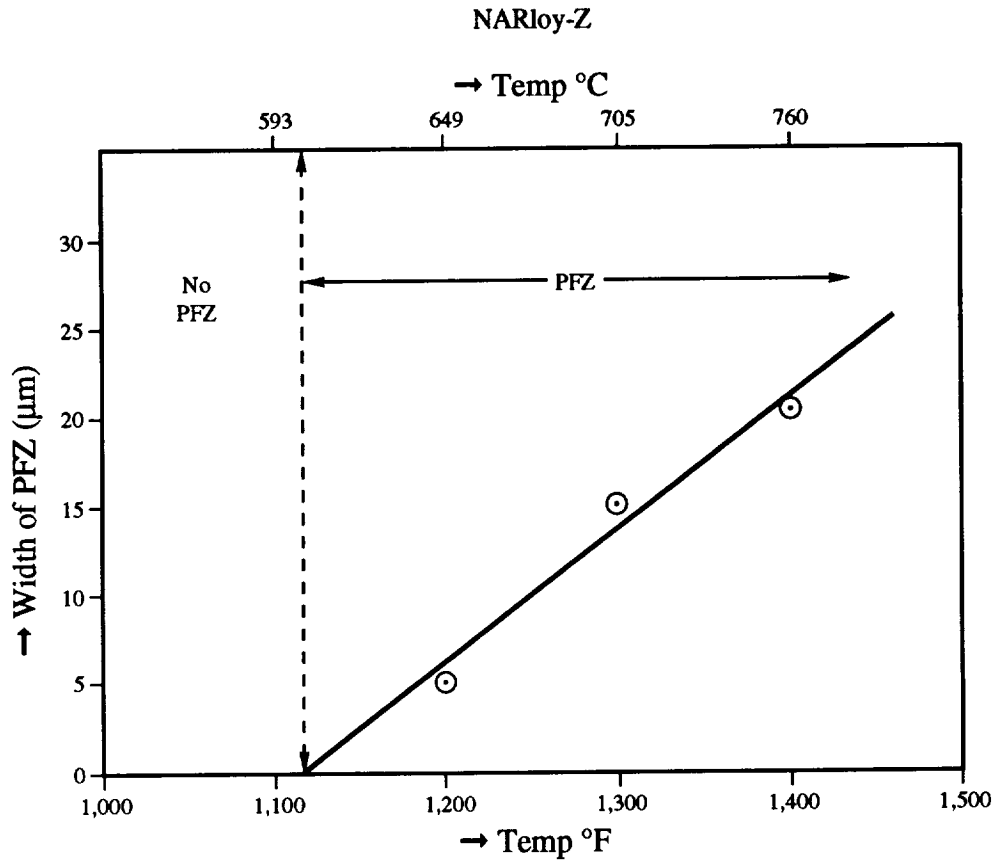


Figure 15. Plot of PFZ width as a function of exposure to temperatures ranging from 649 to 760 °C (1,200 to 1,400 °F).

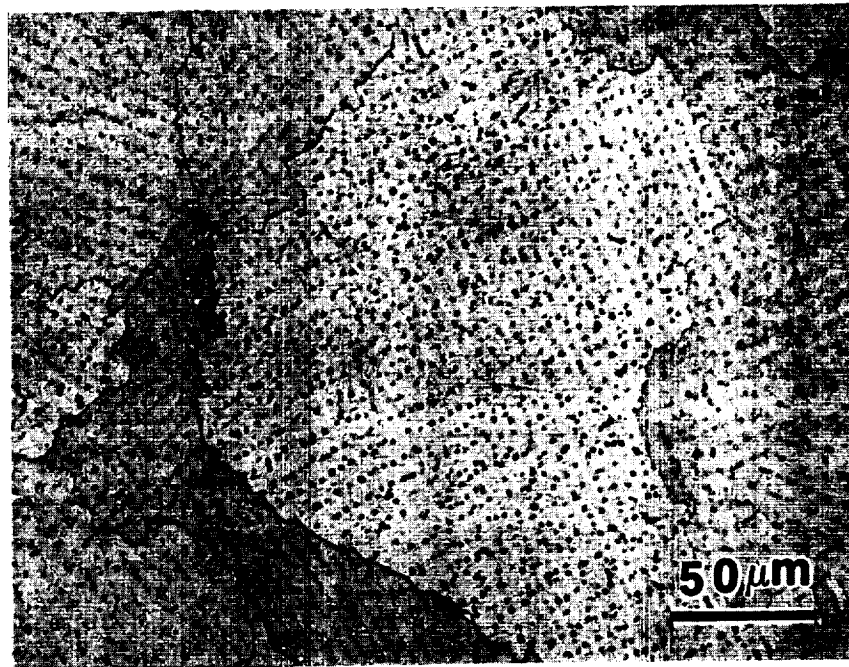


Figure 16. Laser-glazed NARloy-Z showing uniform distribution of second phases in Cu matrix.

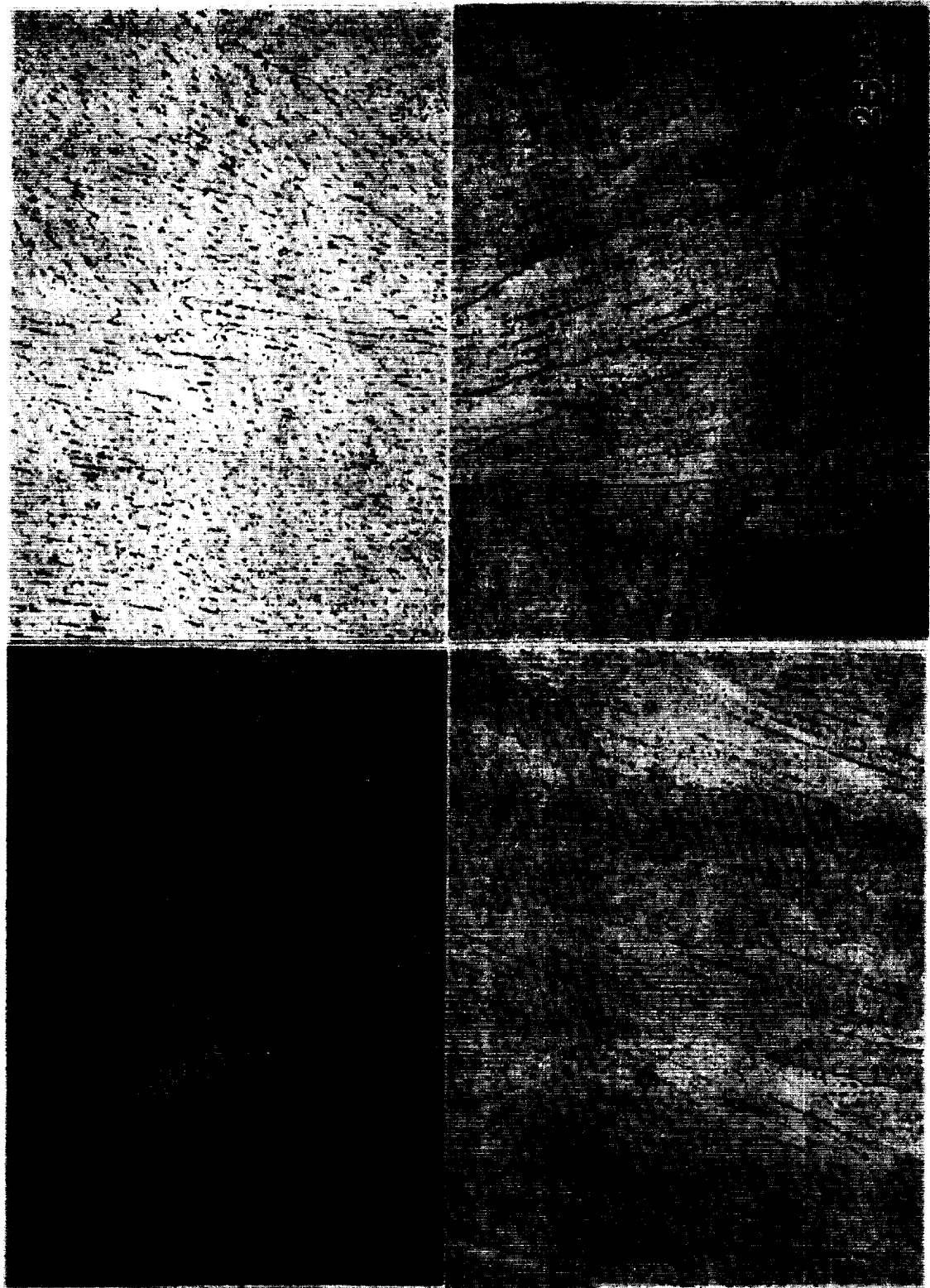


Figure 17. Laser-glazed NARloy-Z showing uniform distribution of second phases in Cu matrix after exposure at 593 °C (1,100 °F) for (a) 24, (b) 48, (c) 72, and (d) 84 h.

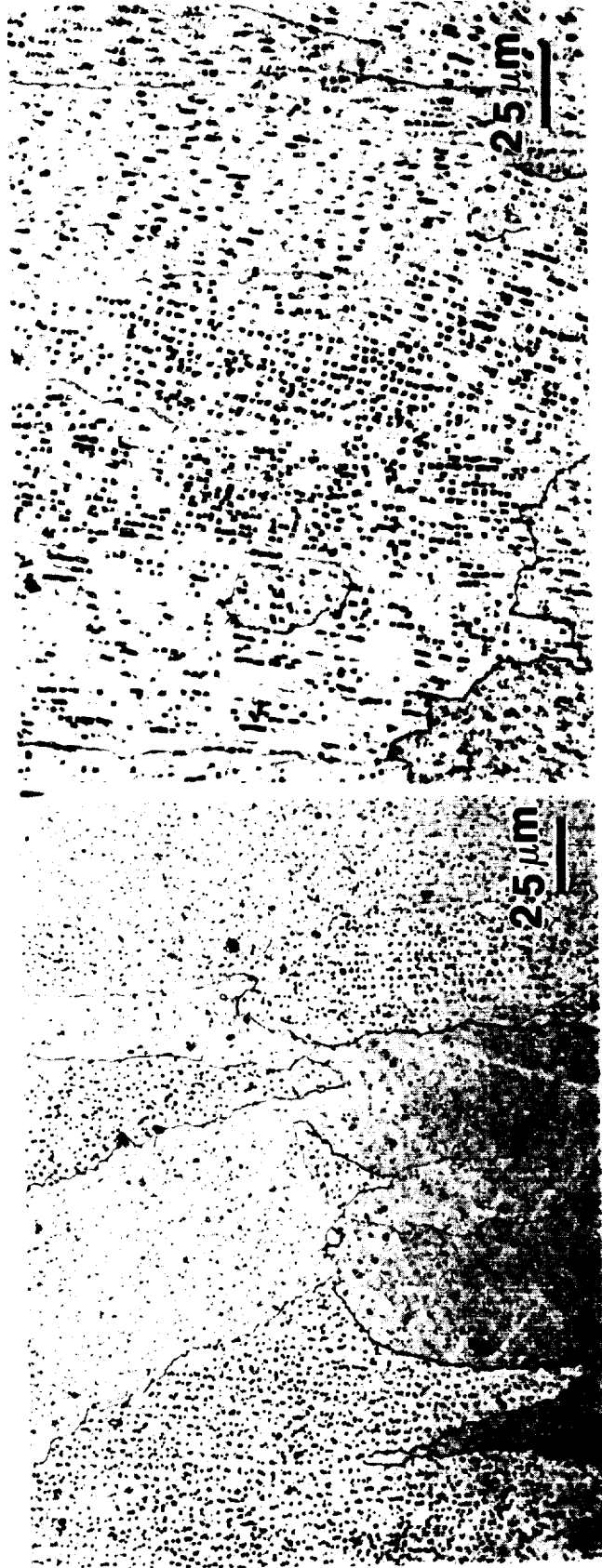


Figure 18. Laser-glazed NARloy-Z showing uniform distribution of faceted second phases in Cu matrix after exposure at 649 °C (1,200 °F) for (a) 24 and (b) 48 h.

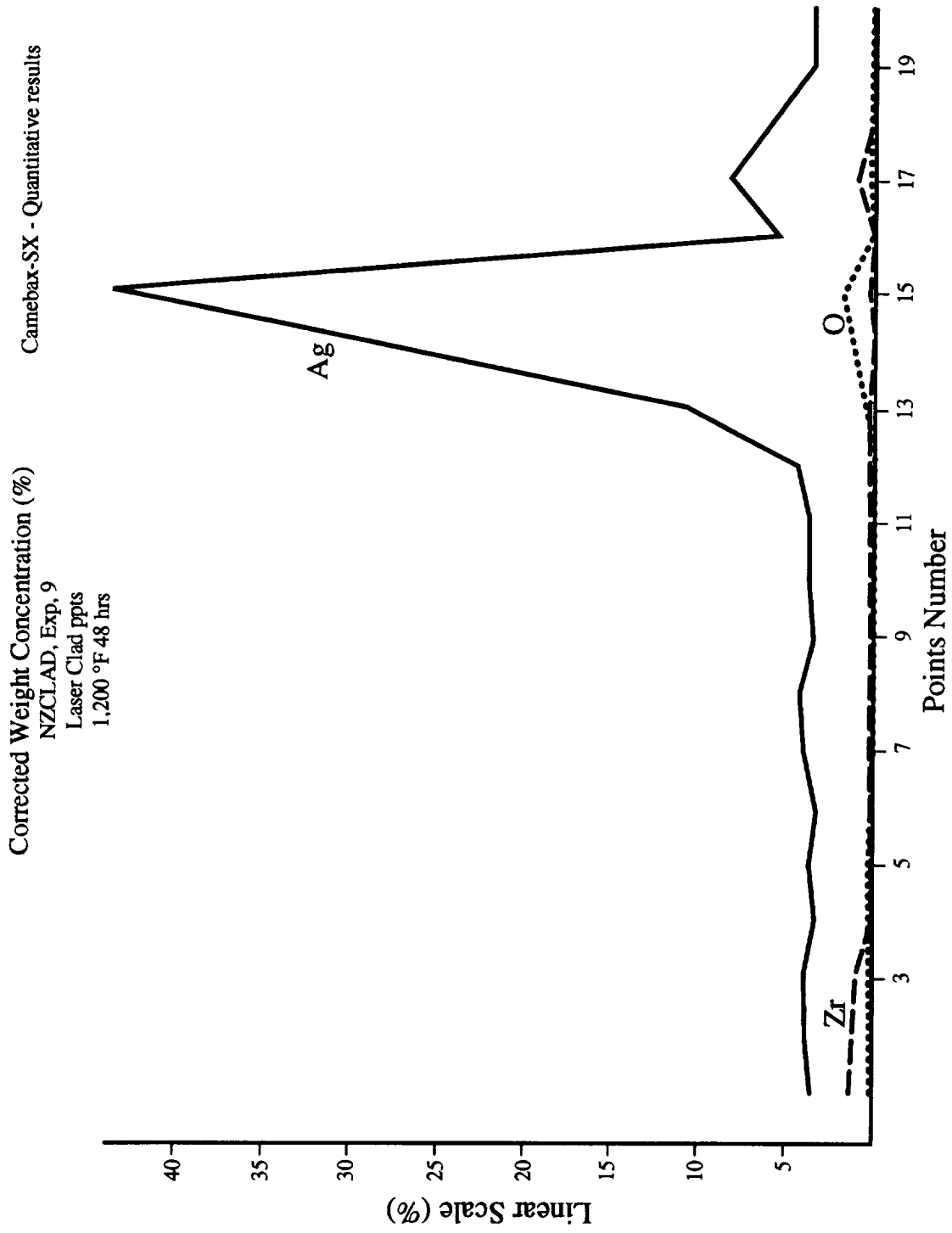


Figure 19. EPMA across the faceted precipitate, as marked in figure 18.

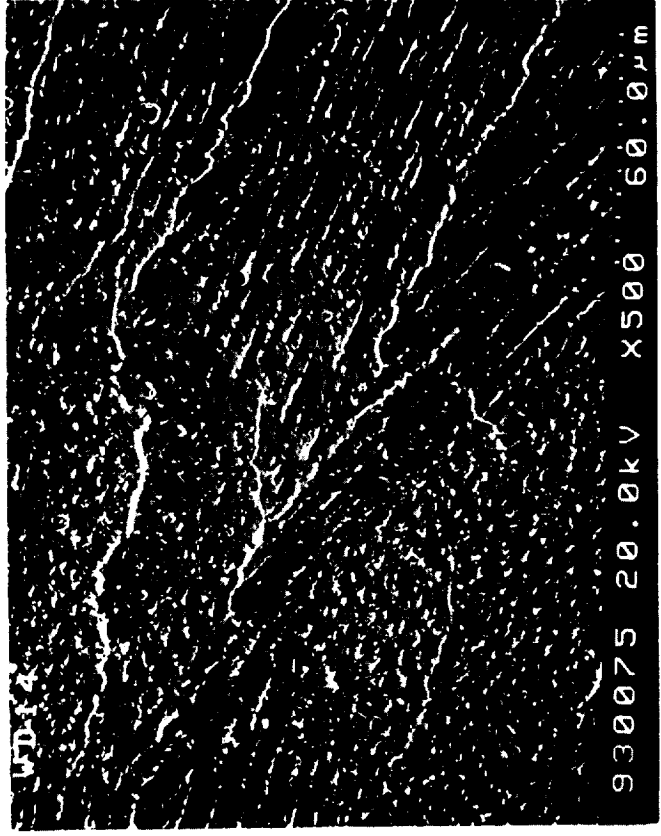


Figure 20. Laser-glazed NARloy-Z showing uniform distribution of second phases in Cu matrix after 24 h at 649 °C (1,200 °F).

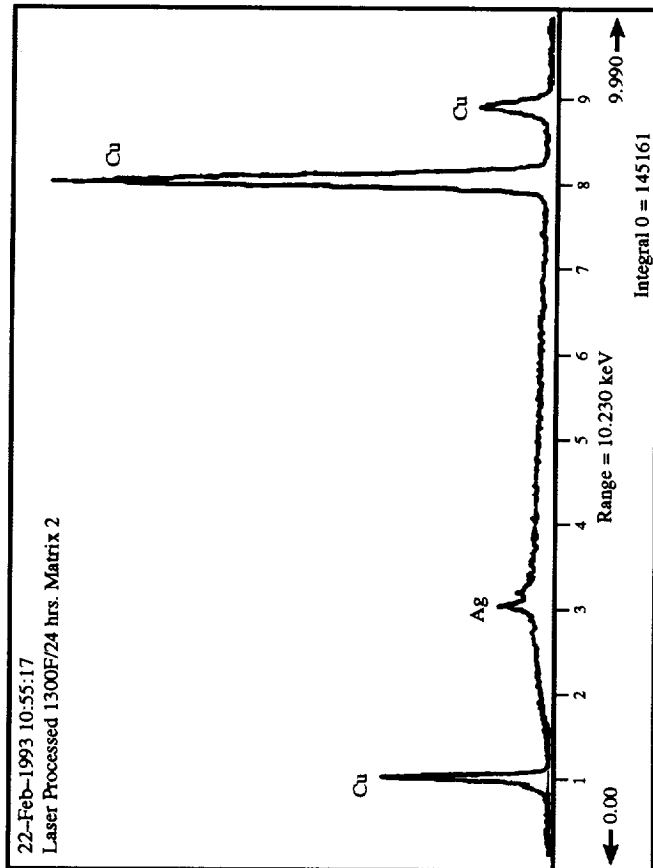
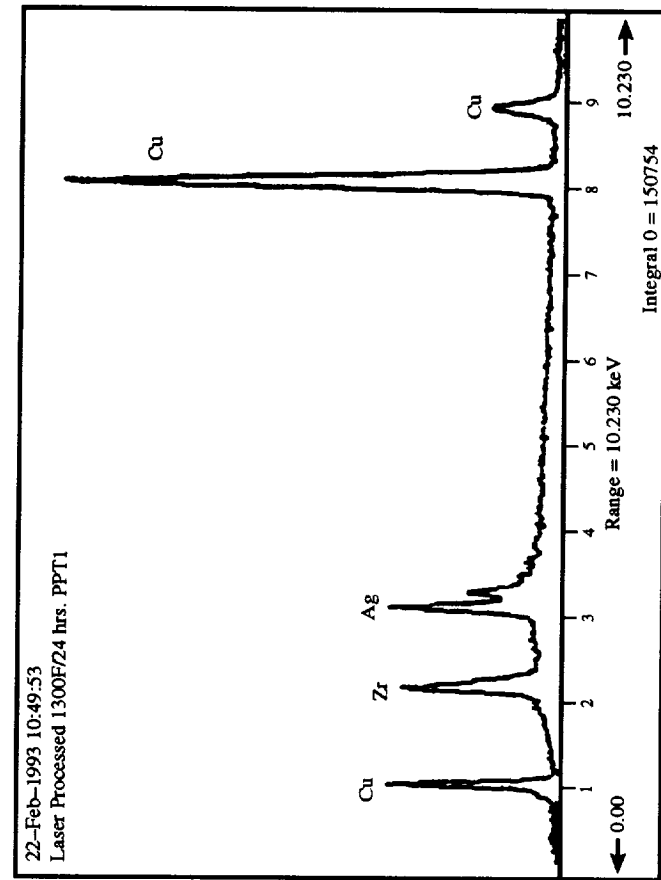


Figure 21. EDS spectrum of precipitate and matrix from figure 20.



Figure 22. Laser-glazed NARloy-Z showing uniform distribution of second phases in Cu matrix after exposure at 760 °C (1,400 °F) for (a) 24 and (b) 48 h.

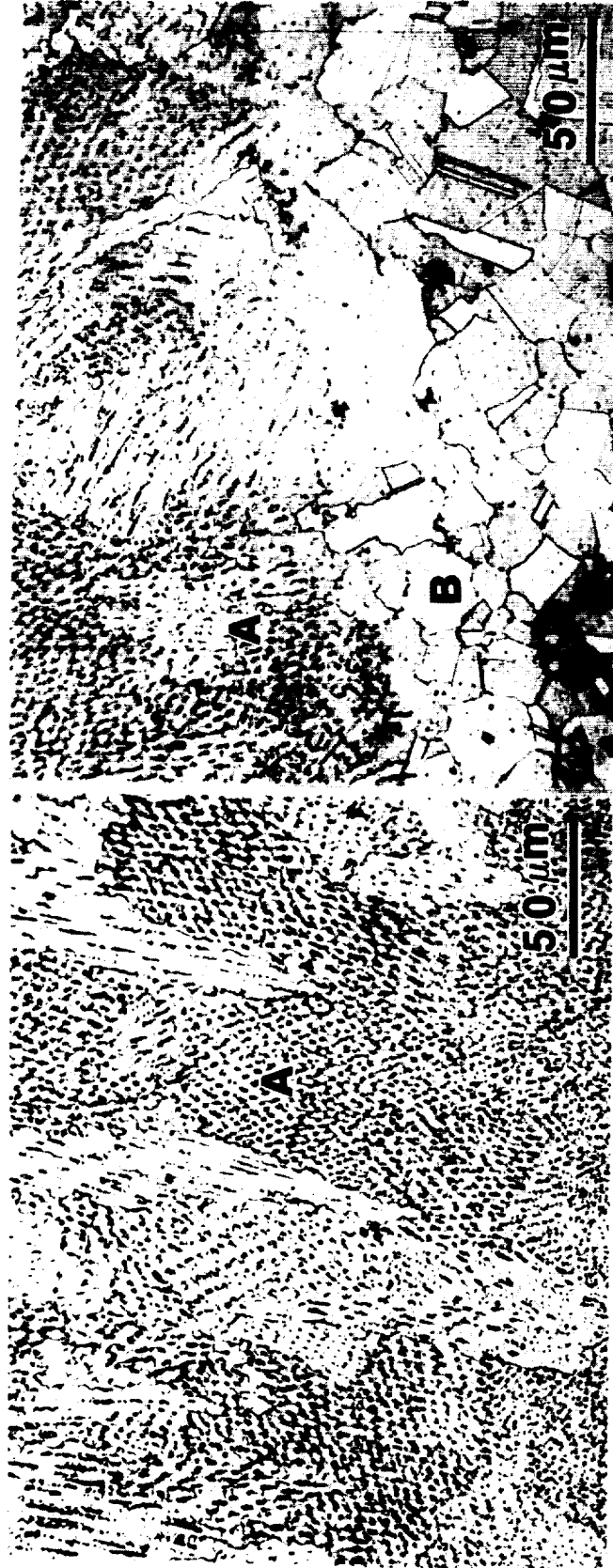


Figure 23. Electron beam-glazed NARloy-Z with uniform distribution of second phases in Cu matrix at a melt depth of ~0.6 mm (25 mils).

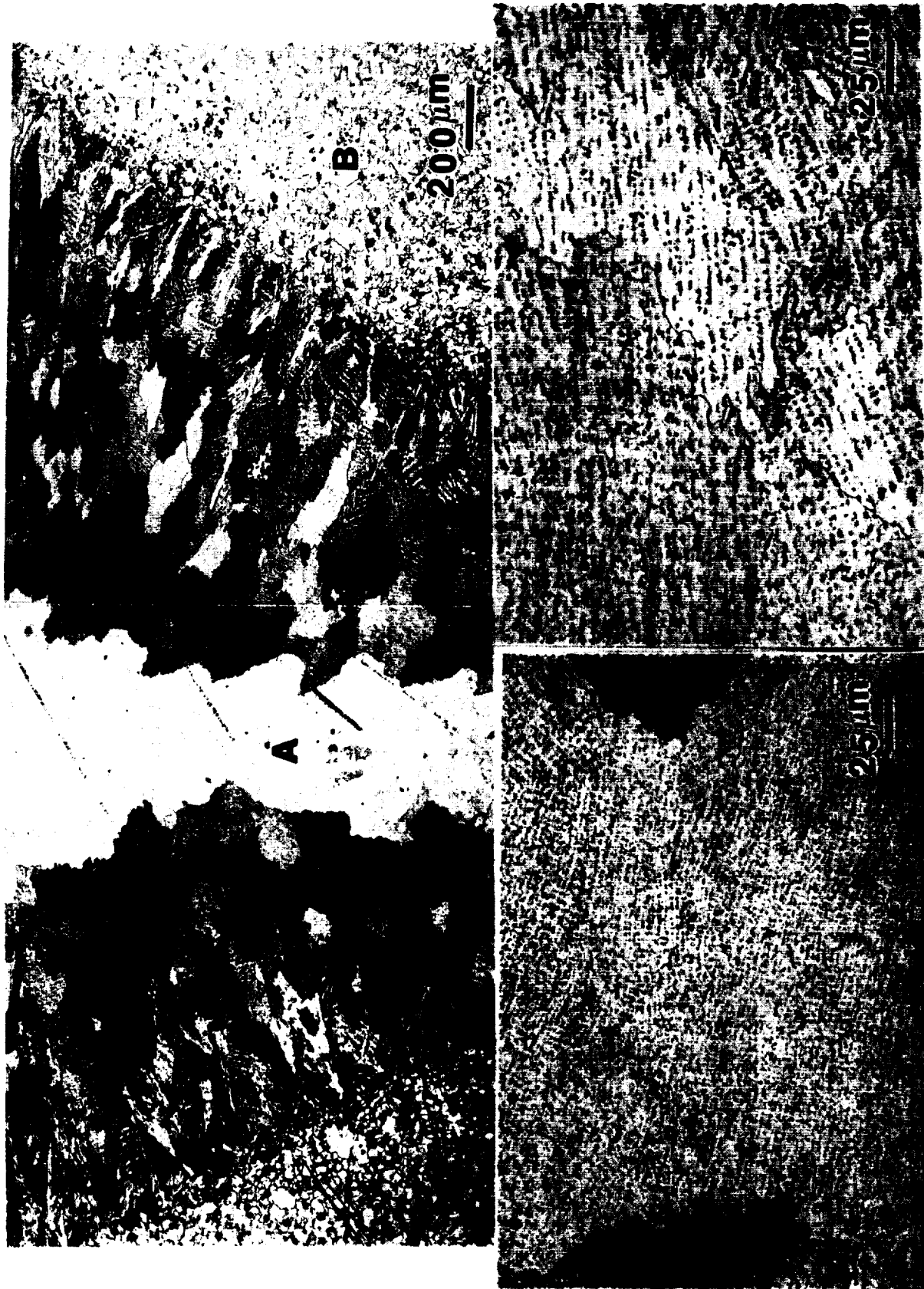


Figure 24. Electron beam beam-glazed NARloy-Z showing uniform distribution of second phases in Cu matrix at melt depth of ~2 mm (80 mils).

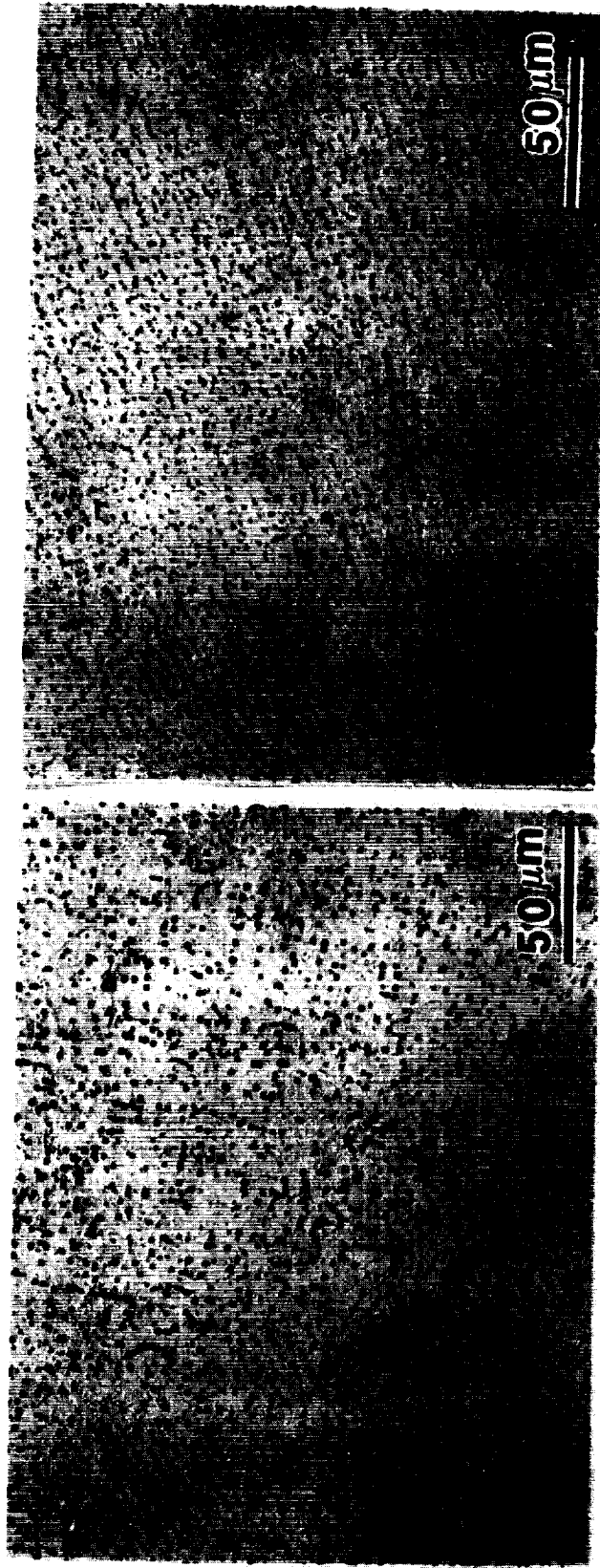



Figure 25. Electron beam-glazed NARloy-Z showing uniform distribution of faceted second phases in Cu matrix after 24 h at (a) 705 °C (1,300 °F) and (b) 760 °C (1,400 °F).

APPROVAL

MICROSTRUCTURAL STABILITY OF WROUGHT, LASER AND ELECTRON BEAM GLAZED NARLOY-Z ALLOY AT ELEVATED TEMPERATURES

By J. Singh, G. Jerman, B. Bhat, and R. Poorman

The information in this report has been reviewed for technical content. Review of any information concerning Department of Defense or nuclear energy activities or programs has been made by the MSFC Security Classification Officer. This report, in its entirety, has been determined to be unclassified.



P.H. SCHUERER
Director, Materials and Processes Laboratory

